J. Chem. Sci. Vol. 125, No. 6, November 2013, pp. 1435–1443.

Synthesis, optical and thermal behaviour of palladium(II) complexes with 4-(4-alkoxy-2-hydroxybenzylideneamino)azobenzene

BOON-TECK HENG[a], GUAN-YEOW YEAP[a,*] and DAISUKE TAKEUCHI[b]

[a]Liquid Crystal Research Laboratory, School of Chemical Sciences, Universiti Sains Malaysia, 11800 Minden, Penang, Malaysia

[b]Chemical Resources Laboratory (Mailbox R1-03), Tokyo Institute of Technology, 4259 Nagatsuta, Midori-ku, Yokohama, 226-8503, Japan

e-mail: gyyeap@usm.my

MS received 6 April 2013; revised 18 August 2013; accepted 21 August 2013

Abstract. A series of new Pd(II) complexes derived from the reaction of palladium acetate with 4-(4-alkoxy-2-hydroxybenzylideneamino)azobenzene having the flexible terminal chain of OC_nH_{2n+1}, in which n are even numbers ranging from 8 to 16, has been successfully synthesized. The physical measurement and spectroscopic techniques (FTIR and ^{1}H-NMR) reveal that the Pd(II) complexes possess the Pd–N and Pd–O coordination modes in which the central Pd(II) adopts square-planar geometry. The observation under the polarized light shows that all the ligands and Pd(II) complexes exhibit enantiotropic mesophases. The ligands with n-octyloxy and n-decyloxy flexible chains exhibit the nematic (N) and smectic A (SmA) phases whilst the Pd(II) complexes show exclusive SmA phase. The SmA phase observed in Pd(II) complexes can be supported by the presence of focal conic fan-shaped texture with the presence of curved lines which are prominent during the cooling process. On the other hand, the comparison studies show that Pd(II) complexes possess exceptional higher phase transition temperatures as compared to the corresponding Cu(II) and Ni(II) complexes.

Keywords. Pd(II) complexes; smectic A; nematic; ^{1}H-NMR; Cu(II) complexes.

1. Introduction

Metallomesogens are commonly referred to the coordination compounds which include the complexes containing mesogenic or non-mesogenic ligands, salt of organic acids or certain organometallic compounds possessing s, p, d and f block metals.[1] The last ten years have seen a steady increase in the interest towards these metallomesogens and the recognition of their potential as advanced materials.[2] One of the reasons making these metallomesogen so essential in the technological advancement is the ultimate shapes associated with various geometries of the central metal atom or ion ranging from square planar, folder square, lantern, pyramidal and octahedral geometrical shapes.[3,4] From the chemical and physical viewpoints, the central metal ions can enhance the richness in oxidation state, colour and magnetism.[5]

Among these materials, the azo-based polymeric liquid crystals or metallomesogens containing uncomplexed azo moieties has been given more attention. In general, the metallomesogens containing the uncomplexed azo moieties are capable of changing the molecular shape by the reversible *cis–trans* isomerization under the influence of UV or photoirradiation. These materials are useful particularly in the development of information recording system such as high-density optical data storage, optical switching, display and nonlinear optics.[6,7] Another interesting feature of these compounds lies on its potential to form rod-like molecules leading to the liquid crystalline properties.[8]

Rezvani and co-workers had earlier reported the synthesis and liquid crystalline properties of some metallomesogens containing isomerizable azo moieties wherein the metal ion such as Cu(II), Ni(II) and VO(IV) are widely used in formulating the novel metallomesogenic system.[9,10] In 2002, Nandiraju and co-workers reported the influence of metal ion on the mesomorphic properties of the ligands.[11] Similar studies had been carried out by Suste and co-workers.[5] In spite of these studies, the influence of the metal on the mesophase and correlation of the structure with the anisotropic properties of metallomesogens are still subject to further investigation.

Recently, we have reported the synthesis and liquid crystalline character of Cu(II) and Ni(II) complexes

*For correspondence

with ligands derived from azobenzene-cored Schiff base.[12,13] Thus, in this work, we report the synthesis and liquid crystalline properties of new *bis*[4-(4-alkoxy-2-hydroxybenzylideneamino)azobenzene]palladium(II) homologous compounds (scheme 1). Besides, the differences among the ultimate complexes in terms of their optical and thermal behaviour are also studied and reported.

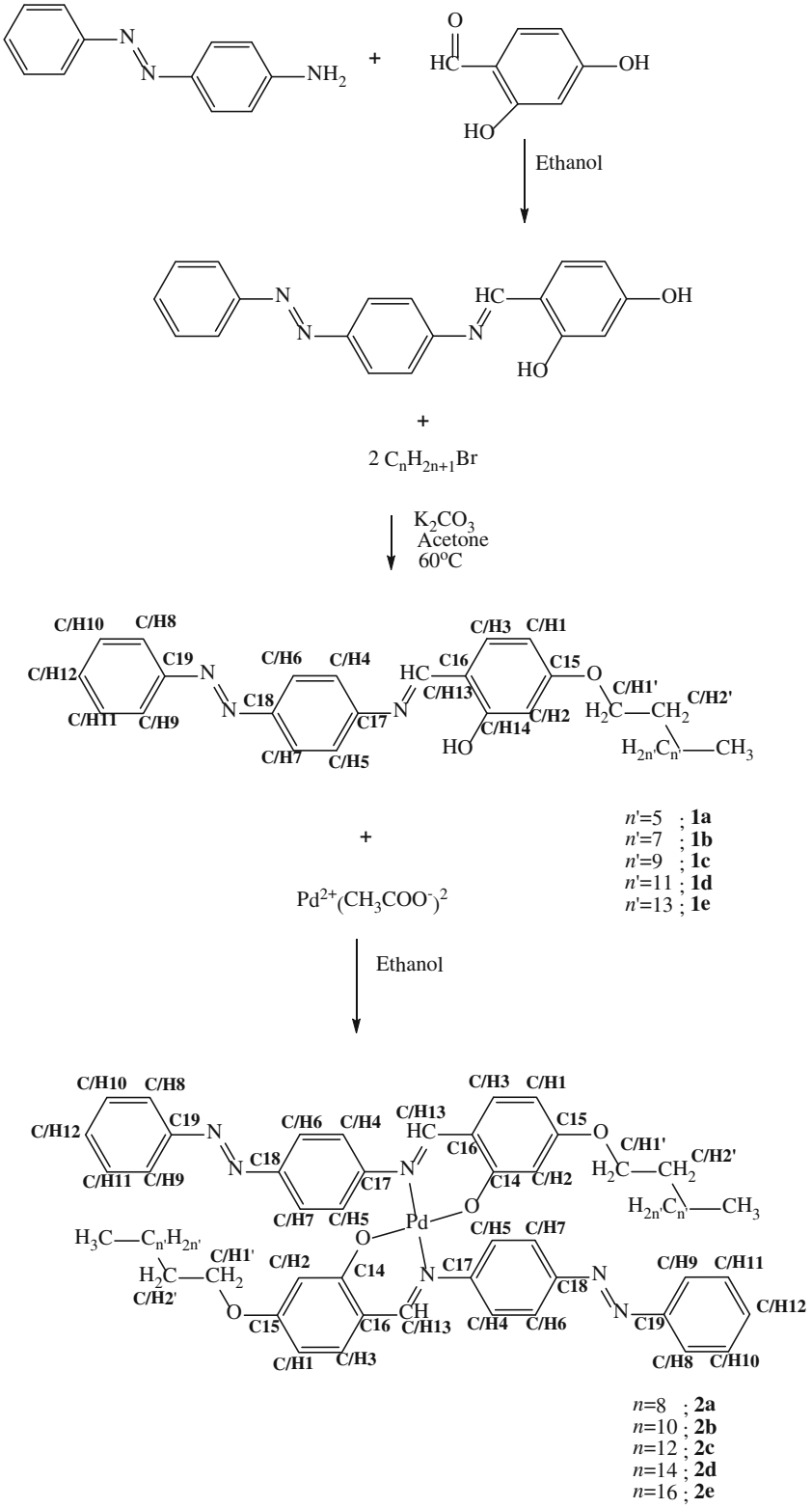

Scheme 1. Synthetic routes toward formation of ligands **1a**–**1e** and Pd(II) complexes **2a**–**2e**.

2. Experimental

2.1 *Materials*

Potassium carbonate was purchased from Systerm while 2,4-dihydroxybenzaldehyde was obtained from Acros Organic. 1-Bromooctane, 1-bromodecane, 1-bromododecane, 1-bromotetradecane, 1-bromohexadecane and palladium(II) acetate were purchased from Merck whereas 4-aminoazobenzene was purchased from Aldrich-Chemical. All reagents mentioned above are used without further purification.

2.2 *Physical measurements*

The ^{1}H-NMR spectra were obtained by using Brucker Avance 400 MHz ultrashield spectrometers equipped with ultrashield magnet. Deuterated chloroform ($CDCl_3$) and dimethysulphoxide (DMSO-d_6) were used as solvent and TMS as internal standard. The FTIR spectra were recorded using a Perkin Elmer 2000-FTIR spectrophotometer in the frequency range 4000–400 cm^{-1} with sample prepared in KBr disc. Elemental (C, H and N) analysis were carried out using a Perkin Elmer 2400 LS Series CHNS/O analyzer. The phase transition temperatures and enthalpy values were measured by using a Seiko DSC6200R calorimeter with the heating and cooling rate of ± 5°C. The optical observations were made with a Carl Zeiss Axioskop 40 polarizing microscope equipped with a Linkam LTS 350 hot stage and TMS94 temperature controller. The samples studied by optical microscope were prepared in thin film sandwiched between glass slide and cover.

2.3 *Synthesis of 4-(4-alkoxy-2-hydroxybenzylideneamino) azobenzene,* ***1a–1e***

The synthesis of 4-(4-alkoxy-2-hydroxybenzylideneamino)azobenzene, **1a**–**1e** follows the method similar to that reported earlier.[12,13]

2.4 *Synthesis of the Pd(II) complexes* ***2a–2e***

An ethanolic solution (10 mL) of palladium(II) acetate (1.0 mmol) was added drop-wise to a hot ethanolic solution (50 mL) of ligands **1** (1.0 mmol) in round bottom flask. The mixture solution was refluxed for 6 h and then cooled to room temperature. The dark green precipitate was collected by filtration and recrystallized from ethanol.

2a: Dark green, yield 82%. Elemental analysis/%: Found C 67.59, H 6.42, N 8.60; calculated ($C_{54}H_{60}N_6O_4Pd$), C 67.36, H 6.23, N 8.73. IR (KBr)υ_{max}/cm^{-1}: 1206 (C–O ether), 1309 (C–O phenolic), 1470 (N=N), 1587 (C=C), 1605 (C=N), 2921–2850 (C-H alkyl). ^{1}H NMR (400 MHz, $CDCl_3$), δ (ppm): 6.17 (dd, H1, J = 12 Hz), 5.55 (s, H2), 7.08 (d, H3, J = 12 Hz), 7.48–7.62 (m, H4, H5, H10, H11, H12), 8.02 (d, H6, H7, J = 8 Hz), 7.97 (dd, H8, H9, J = 4 Hz), 7.66 (s, H13), 3.67 (t, H1′, J = 4 Hz), 1.20–1.64 (m, H2′-H7′), 0.89 (t, H8′, J = 8 Hz). ^{13}C NMR (75 MHz, $CDCl_3$), δ (ppm): 107.70 (C1), 102.33 (C2), 135.91 (C3), 123.83 (C4,C5), 125.04 (C6,C7), 123.88 (C8, C9), 129.61 (C10,C11), 131.41 (C12), 153.10 (C13), 161.10 (C14), 165.87 (C15), 114.90 (C16), 152.57 (C17), 151.12 (C18), 151.35 (C19), 68.22 (C1'), 32.31-23.10 (C2'-C7'), 14.53 (C8).

2b: Dark green, yield 81%. Elemental analysis/%: Found C 68.56, H 6.92, N 8.14; calculated ($C_{58}H_{68}N_6O_4Pd$), C 68.37, H 6.67, N 8.25. IR (KBr)υ_{max}/cm^{-1}: 1206 (C–O ether), 1310 (C–O phenolic), 1469 (N=N), 1588 (C=C), 1606 (C=N), 2923–2852 (C-H alkyl). ^{1}H NMR (400 MHz, $CDCl_3$), δ (ppm): 6.17 (dd, H1, J = 12 Hz), 5.56 (s, H2), 7.09 (d, H3, J = 12 Hz), 7.49–7.63 (m, H4, H5, H10, H11, H12), 8.02 (d, H6, H7, J = 8 Hz), 7.96 (dd, H8, H9, J = 4 Hz), 7.65 (s, H13), 3.67 (t, H1′, J = 4 Hz), 1.19–1.63 (m, H2′-H9′), 0.89 (t, H10′, J = 8 Hz). ^{13}C NMR (75 MHz, $CDCl_3$), δ (ppm): 107.70 (C1), 102.34 (C2), 135.97 (C3), 123.82 (C4,C5), 125.09 (C6,C7), 123.87 (C8, C9), 129.61 (C10,C11), 131.40 (C12), 153.15 (C13), 161.08 (C14), 165.88 (C15), 114.91 (C16), 152.57 (C17), 151.13 (C18), 151.34 (C19), 68.22 (C1'), 32.31–23.10 (C2'-C7'), 14.54 (C8).

2c: Dark green, yield 83%. Elemental analysis/%: Found C 69.53, H 7.31, N 7.72; calculated ($C_{62}H_{76}N_6O_4Pd$), C 69.27, H 7.07, N 7.82. IR (KBr)υ_{max}/cm^{-1}: 1206 (C–O ether), 1310 (C–O phenolic), 1469 (N=N), 1587 (C=C), 1606 (C=N), 2924–2852 (C-H alkyl). ^{1}H NMR (400 MHz, $CDCl_3$), δ (ppm): 6.17 (dd, H1, J = 12 Hz), 5.56 (s, H2), 7.09 (d, H3, J = 12 Hz), 7.49–7.63 (m, H4, H5, H10, H11, H12), 8.02 (d, H6, H7, J = 8 Hz), 7.97 (dd, H8, H9, J = 4 Hz), 7.66 (s, H13), 3.67 (t, H1′, J = 4 Hz), 1.19–1.63 (m, H2′-H11′), 0.90 (t, H12′, J = 8 Hz). ^{13}C NMR (75 MHz, $CDCl_3$), δ (ppm): 107.70 (C1), 102.34 (C2), 135.95 (C3), 123.82 (C4,C5), 125.04 (C6,C7), 123.88 (C8,C9), 129.61 (C10,C11), 131.42 (C12), 153.14 (C13), 161.10 (C14), 165.87 (C15), 114.90 (C16), 152.58 (C17), 151.13 (C18), 151.35 (C19), 68.22 (C1'), 32.31-23.10 (C2'-C7'), 14.53 (C8).

2d: Dark green, yield 79%. Elemental analysis/%: Found C 70.31, H 7.67, N 7.38; calculated

($C_{66}H_{84}N_6O_4Pd$), C 70.10, H 7.43, N 7.43. IR (KBr)υ_{max}/cm^{-1}: 1206 (C–O ether), 1309 (C–O phenolic), 1470 (N=N), 1589 (C=C), 1605 (C=N), 2922–2851 (C-H alkyl). ^{1}H NMR (400 MHz, $CDCl_3$), δ (ppm): 6.53 (dd, H1, J = 12 Hz), 5.56 (s, H2), 7.09 (d, H3, J = 12 Hz), 7.49–7.62 (m, H4, H5, H10, H11, H12), 8.02 (d, H6, H7, J = 8 Hz), 7.96 (dd, H8, H9, J = 4 Hz), 7.66 (s, H13), 3.67 (t, H1', J = 4 Hz), 1.20–1.63 (m, H2'-H13'), 0.91 (t, H14', J = 8 Hz). ^{13}C NMR (75 MHz, $CDCl_3$), δ (ppm): 107.72 (C1), 102.35 (C2), 135.92 (C3), 123.81 (C4,C5), 125.05 (C6,C7), 123.88 (C8,C9), 129.63 (C10,C11), 131.41 (C12), 153.12 (C13), 161.09 (C14), 165.89 (C15), 114.92 (C16), 152.58 (C17), 151.12 (C18), 151.33 (C19), 68.21 (C1'), 32.31–23.09 (C2′-C7′), 14.54 (C8).

2e: Dark green, yield 85%. Elemental analysis/%: Found C 71.08, H 8.05, N 6.95; calculated ($C_{70}H_{92}N_6O_4Pd$), C 70.83, H 7.75, N 7.08. IR (KBr)υ_{max}/cm^{-1}: 1206 (C–O ether), 1309 (C–O phenolic), 1469 (N=N), 1589 (C=C), 1605 (C=N), 2920–2851 (C-H alkyl). ^{1}H NMR (400 MHz, $CDCl_3$), δ (ppm): 6.16 (dd, H1, J = 12 Hz), 5.56 (s, H2), 7.09 (d, H3, J = 12 Hz), 7.49–7.62 (m, H4, H5, H10, H11, H12), 8.02 (d, H6, H7, J = 8 Hz), 7.97 (dd, H8, H9, J = 4 Hz), 7.66 (s, H13), 3.67 (t, H1′, J = 4 Hz), 1.20–1.64 (m, H2′-H15′), 0.89 (t, H16′, J = 8 Hz). ^{13}C NMR (75 MHz, $CDCl_3$), δ (ppm): 107.71 (C1), 102.33 (C2), 135.91 (C3), 123.83 (C4,C5), 125.05 (C6,C7), 123.87 (C8,C9), 129.62 (C10,C11), 131.41 (C12), 153.10 (C13), 161.10 (C14), 165.87 (C15), 114.92 (C16), 152.56 (C17), 151.12 (C18), 151.35 (C19), 68.20 (C1'), 32.31–23.10 (C2'-C7'), 14.53 (C8).

3. Results and discussion

3.1 *Synthesis*

Ligands **1a**–**1e** were obtained from the condensation between aromatic amine and 2,4-dihydroxybenzaldehyde wherein the imine thus obtained was alkylated by various bromoalkane ($C_nH_{2n+1}Br$; where n = 8−16) via the Williamson etherification. The reactions between **1a** and **1e** with Pd(II) acetate in stoichiometric ratio have led to the formation of Pd(II) complexes **2a**–**2e** as dark green solids. The structure elucidation for compounds **1a**–**1e** and **2a**–**2e** were carried out by FT-IR, ^{1}H-NMR and elemental analysis. The physical properties of the compounds thus obtained are summarized in experimental section. These data show that the empirical formula are in accordance with all the complexes **2a**–**2e** of which the ratio of Pd(II) to ligands is 1:2.

From the FTIR data of ligands **1a**–**1e** and corresponding Pd(II) complexes **2a**–**2e**, it can be observed that the broad band assignable to the O–H stretching in the free ligands disappears upon complexation with Pd(II) indicating that the OH group is deprotonated. As such, the ligand is coordinated to the metal ion via the anionic O^-.[1,9,10,14] Furthermore, the coordination of O to Pd(II) ion is further supported by the stretching vibration of phenolic C–O which has shifted to a higher frequency at 1309–1310 cm^{-1} as compared to 1280–1285 cm^{-1} in uncoordinated ligands.[15,16] Comparing the stretching frequency of azomethine C=N in the free ligand (1624–1625 cm^{-1}) and that in Pd(II) complexes (1605–1606 cm^{-1}) suggests the coordination of non-bonding electron on N atom to central Pd(II) ion. This observation can be ascribed to the reduction of double bond character of the C=N bond and it is in agreement with the results obtained from other analogous complexes.[5,9–11,14,17,18] Besides, a weak band at 1471–1473 cm^{-1} indicates the stretching frequency of azolinkages of N=N.[19] Since this band is not shifted upon complex formation, therefore, the coordination of the N atom from the azo-linkages to Pd(II) ion can be ruled out. All of these observations support the formation of Pd–O and Pd–N coordination modes in which the ratio of Pd(II) to ligands is 1:2.

The investigation by the ^{1}H-NMR chemical shifts (δ) shows that the signals for H1 and H2 (δ 6.51–6.55 ppm), H3 (δ 7.30–7.33 ppm) and H13 (δ 8.62–8.63 ppm) in uncoordinated ligands **1a**–**1e** are shifted upfield upon complexation. The upfield shift of proton signals shows the increase of shielding effect which can be explained by the nature of the molecular structures of **2a**–**2e** wherein the Pd(II) ion is stabilized by Pd–O and Pd–N coordination modes. The stabilization has further been enhanced through the existence of back bonding from Pd(II) ion to the conjugated system consisting of H1, H2, H3 and H13.[20] Besides, the overlapping of chemical shifts for proton H1 and H2 in uncoordinated ligands is not observed in Pd(II) complexes. These two protons have shifted to upper field giving rise to two separate peaks. The large upfield shift in the chemical shift of azomethine proton H13 has further substantiated the coordination of N atom from the ligands to the central Pd(II) ion.[17,18,20] In addition, the absence of a singlet at δ = 13.60 ppm indicates that OH group is deprotonated prior to form new coordination mode of Pd–O. The ^{13}C-NMR chemical shifts (δ) for azomethine carbon (C13) and OH group carbon of C14 also support the presence of new coordination mode of Pd–O whereby the chemical shift of C13 and C14 at respective δ = 162.38−162.40 ppm and δ = 164.48 − 164.56 ppm were shifted

Table 1. Phase transition temperature (°C) and associated enthalpy (kJ mol^{-1}) given in parenthesis of ligands **1a**–**1d**.

Ligands		Cr_1		Cr_2		SmA	N		I
1a	Heating	•	74.2 (5.4)	•	109.7 (30.5)	•	164.3[a]	•	176.5[a] •
	Cooling	•	76.1 (−23.5)			•	161.1[a]	•	173.9[a] •
1b	Heating	•	99.6 (7.7)	•	107.1 (27.7)	•	166.9[a]	•	168.5 (3.3) •
	Cooling	•	80.7 (−31.7)			•	159.4[a]	•	162.6[a] •
1c	Heating	•			106.8 (36.3)	•			165.1 (3.2) •
	Cooling	•			96.1 (−34.3)	•			168.2 (−3.6) •
1d	Heating	•			110.3 (64.2)	•			167.9 (6.5) •
	Cooling	•			91.5 (−66.1)	•			164.6 (−6.0) •

Cr, crystal; N, nematic; Sm A, smectic A; I, isotropic
[a]Denotes transition temperature derived from unresolved peaks
Dot means the presence of the phase

to 153.10–153.15 ppm and 161.08–161.10 ppm upon complex formation.

The central Pd(II) ion in respective complexes **2a**–**2e** is stabilized by the two equivalent ligands in which the palladium ion possesses square planar geometry. This can be supported by the ^{1}H-NMR spectra in which no peak broadening was detected. This observation is in agreement with that reported by Blackburn and co-workers in which they found that the tetrahedral geometry of metal complexes caused the peaks broadening whereas the square planar analogues prevented the peak broadening.[19] In addition, the square planar geometries of Pd(II) in complexes **2a**–**2e** can be further evident by their common stereochemistry as reported by Hudson and co-workers.[21]

3.2 *Liquid crystalline properties*

The liquid-crystalline properties of ligands **1a**–**1e** with their corresponding Pd(II) complexes have been studied by polarizing optical microscope (POM) equipped with a heating and cooling hot stage and their enthalpy values are obtained by differential scanning calometry (DSC). The respective phase transition temperatures and enthalpy values for ligands **1a**–**1e** and Pd(II) complexes **2a**–**2e** are illustrated in tables 1 and 2. All ligands with their corresponding Pd(II) complexes exhibit enantiotropic mesophase. The homologous ligands with $n = 8$ (**1a**) and $n = 10$ (**1b**) show the schlieren and the focal conic fan-shaped textures characteristic of nematic (N) and smectic A (SmA) phases, respectively. However, the N phase is not observed upon further lengthening of the alkoxy chain from ligand **1c** ($n = 12$) to ligand **1e** ($n = 16$). Instead, ligands **1c**–**1e** exhibit only enantiotropic SmA phase. The existence of SmA in ligands **1a**–**1e** have earlier been proven by X-ray diffraction.[12]

Optical observation shows that the whole homologous series of Pd(II) complexes **2a**–**2e** exhibit SmA phase. Upon heating with the transition rate of

Table 2. Phase transition temperature (°C) for complexes **2a**–**2e.**

Complexes		Cr		SmA		I
2a	Heating	•	256.2	•	261.9	•
	Cooling	•	158.6	•	260.8	•
2b	Heating	•	247.4	•	257.4	•
	Cooling	•	186.5	•	251.4	•
2c	Heating	•	224.5	•	249.2	•
	Cooling	•	74.3	•	238.5	•
2d	Heating	•	215.6	•	236.6	•
	Cooling	•	84.1	•	228.9	•
2e	Heating	•	204.9	•	223.4	•
	Cooling	•	83.3	•	215.4	•

Dot means the presence of the phase

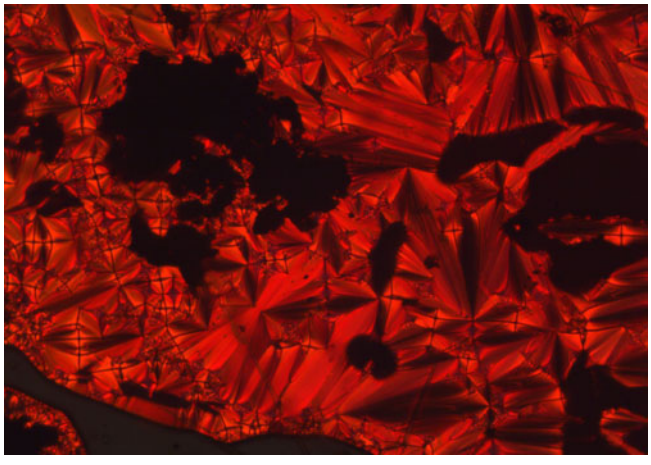

Figure 1. Photomicrograph showing the SmA phase with focal conic fan shape texture of complex **2c** at 224.5°C upon heating.

5°C min^{-1}, these complexes exhibit the SmA phase with focal conic fan-shaped texture as illustrated in figure 1. However, the transition is accompanied by partial decomposition and the continuous heating has led to isotropization.

Upon cooling with the same rate (5°C min^{-1}), the batonnets thus appeared in complex **2c** (figure 2) coalesce to form the SmA phase (figure 3). It is also clearly shown from figure 3 that the focal conic fan-shaped texture filled with curved lines which exist over a large smectogenic temperature range but diminished upon crystallization. As in the Pd(II) complexes **2a**–**2e**, the presence of irregular shape of black spots observed in figures 1, 2 and 3 indicate fast decomposition. Hence, a complete photomicrograph attributed to the presence of SmA phase could not be observed. Besides, the fast decomposition behaviour of Pd(II) complexes has also affected the studies using X-ray diffraction and DSC.

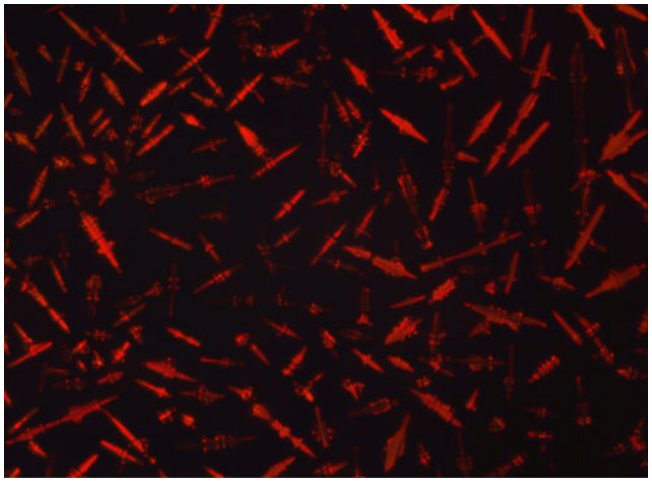

Figure 2. Photomicrograph showing the batonnets of complex **2c** with the presence of arced lines at 242°C during the cooling process.

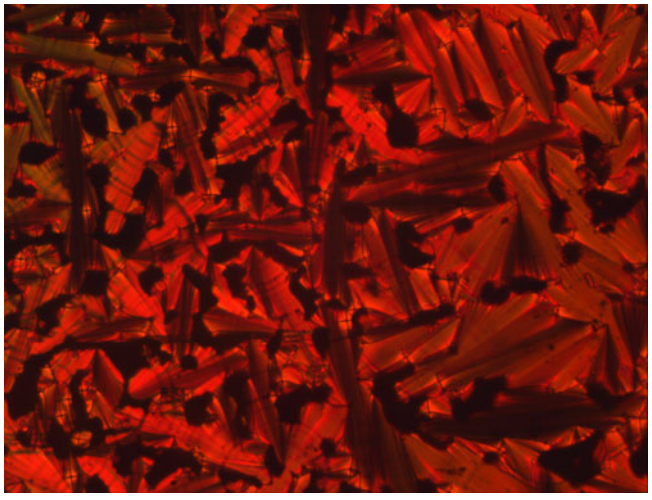

Figure 3. Photomicrograph showing the focal conic fan shape texture of complex **2c** with the presence of arced lines on mesophase upon cooling.

A notable feature among these complexes **2a**–**2e** is that the mesophases thus observed are reproducible upon heating and cooling processes even though these complexes are partially decomposed. However, the presence of arc in the SmA phase is only observed upon cooling process.

Figure 4 illustrates that the Pd complexes **2a** ($n = 8$) and **2b** ($n = 10$) exhibit only SmA phase in comparison to uncoordinated ligands exhibiting both N and smectic A phases. This could plausibly be due to the Pd(II) complexes which posses new coordination modes of Pd–O and Pd–N with greater polarity leading to the suppression of N phase.[5,22] The other factor which enhances the smectogenicity of the complexes can be associated with the increase in the number of aromatic rings in the complexes which has resulted in the lateral interaction between the molecules.[23]

In addition, the correlation study upon heating process shows that the phase transition temperatures (Cr-SmA and SmA-I) of the Pd(II) complexes **2a**–**2e** are relatively higher than those in **1a**–**1e** (figure 4). This indicates that the introduction of Pd(II) increases the phase transition temperature of the corresponding ligands. This observation can be rationalized by the fact that the molecular weights as well as the number of interacting sites of **2a**–**2e** are higher in comparison to the ligands.[3] Further study upon these data also reveals that the transition temperature decreases when the number of carbon atom in the flexible alkoxy chain increases. This can be exemplified by the SmA-I

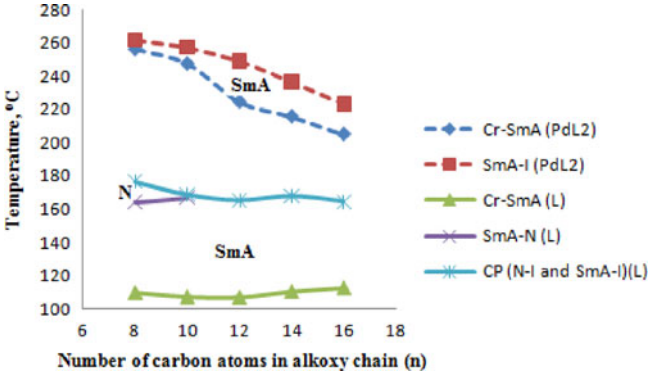

Figure 4. A set of plots of phase transition temperature upon heating versus the number of carbon atoms in alkoxy chain for the ligands **1a**–**1e**, L (solid line) and their Pd(II) complexes, PdL2 (dotted line). Cr, crystal; SmA, Smectic A; N, Nematic; I, Isotropic; CP, Clearing point.

temperature for **2a** (261.9°C) which has decreased to 257.4°C, 249.2°C, 236.6°C and 223.4°C in **2b**, **2c**, **2d** and **2e**, respectively.

3.3 *The comparative study of existing Pd(II) complexes **2a–2e** with earlier reported Cu(II) and Ni(II) complexes.*

In order to rationalize the importance of different metal ion resulted from the liquid crystalline and thermal properties of 4-(4-alkoxy-2-hydroxybenzylidene-amino)azobenzene ligands, the present Pd(II) complexes are compared with our earlier reported Cu(II) and Ni(II) complexes.[12] Below is a summary of the mesophases for ligands **1a–1e** with their corresponding Cu(II), Pd(II) and Ni(II) complexes. All the Pd(II) complexes **2a–2e** show the SmA phase as observed in homologous Cu(II) complexes.[12] However, the coordination of ligands **1a–1e** to Pd(II) metal ion forms a less stable metal complexes which has been evident by the little decomposition of the complexes at melting temperature. In addition, there is obvious variation of the phase transition temperature in Pd(II) complexes as compared to Cu(II) and Ni(II) complexes (figure 5). Figure 5 shows that the Pd(II) complexes have an exceptionally high phase transition temperature. The whole homologous series of Pd(II) complexes have relatively higher transition temperatures of I-SmA as compared to those in Cu(II) complexes. Besides, the clearing temperatures for Pd(II) complexes are also significantly higher as compared to Cu(II) complexes especially for Pd(II) complexes with terminal alkoxy chain from $n = 8$ to $n = 12$. The differences may be due to the difference of the size of metal ion and the possibility of weak metal–metal intermolecular interaction between the complexes.[24]

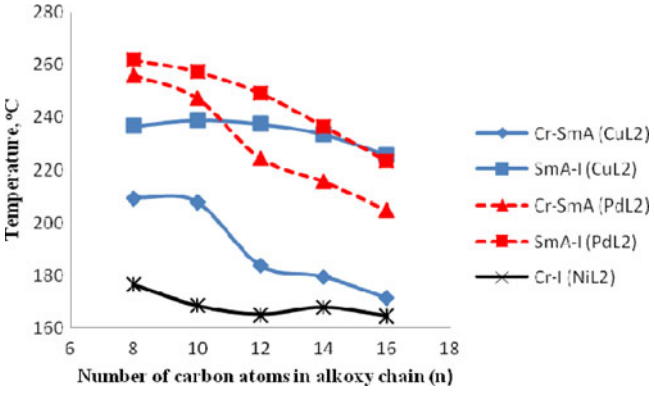

Figure 5. A set of plots of phase transition temperatures upon heating versus the number of carbon atoms in alkoxy chain for the Cu(II), Ni(II) and Pd(II) compexes. Cr, Crystal; SmA, Smectic A; I, Isotopic; CuL2,Cu(II) complexes; NiL2, Ni(II) complexes; PdL2, Pd(II) complexes.

The similar observation in mesomorphic region for Cu(II) and Pd(II) complexes suggests the similar coordination geometry between these two complexes.[12,24] Thus, the Pd(II) complexes are suggested to have square planar geometry according to the common stereochemistry of this kind of compound.[21]

Ligands **1a–1e**

1a and **1b** (n= 8 and 10)

Cr ⟷ SmA ⟷ N ⟷ I

1c, 1d and **1e** (n= 12, 14 and 16)

Cr ⟷ SmA ⟷ I

Cu(II) complexes (n= 8, 10, 12, 14 and 16)

Cr ⟷ SmA ⟷ I

Ni(II) complexes (n= 8, 10, 12, 14 and 16)

Cr ⟷ I

Pd(II) complexes **2a–2e** (n= 8, 10, 12, 14 and 16)

Cr ⟷ SmA ⟷ I

3.4 *The comparative study of different core systems on optical and thermal properties of Pd(II) complexes*

The present Pd(II) complexes series derived from azobenzene-cored Schiff bases ligands **1a–1e** are compared to the structurally related compounds reported by Yeap and co-workers in 2012 with general structure as shown below.[25] Both series have almost similar molecular structure but with different types of cored systems. Thus, general rules for the effect of the chemical constitution in liquid crystalline and thermal properties can be deduced.

The general molecular structure of the two Pd(II) complexes are shown below where Pd(II) complexes **2a–2e** consist of azobenzene-cored system whereas the Pd(II) complexes synthesized by Yeap and co-workers consist of benzothiazole-cored system.[25]

A comparison in term of optical or liquid crystalline properties between the azobenzene-cored Pd(II) complexes **2a–2e** and benzothiazole-cored Pd(II) complexes reveals that the differences are pronounced. All the homologous members of Pd(II) complexes **2a–2e** exhibit enantiotropic SmA phase whereas the DSC traces and optical observation of benzothiazole-cored

Pd(II) complexes show that these complexes are non-liquid crystalline.

However, a comparison with regard to the thermal properties for both Pd(II) complexes show that all the benzothiazole-cored Pd(II) complexes undergo a considerable amount of decomposition right after the isotropic phase. Similarly, all the Pd(II) complexes **2a**–**2e** also exhibit thermal decomposition behaviour. But, these Pd(II) complexes just decompose slightly during the transition from crystal to SmA phase and the SmA phase is reproducible upon the subsequent heating and cooling processes.

The above observations show that azobenzene-cored system favours the mesophase formation and forms Pd(II) complexes **2a**–**2e** which are more stable as compared to the benzothiazole-cored Pd(II) complexes that are fully decomposed. By substituting a core system with another one, the polarity, core length, rigidity and fractional residue volume are also altered. As a consequence, the differences in liquid crystalline and thermal behaviour of these two Pd(II) complexes can be distinguished.

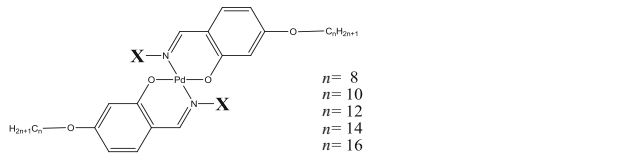

X

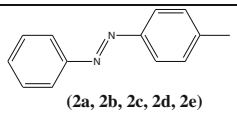

(2a, 2b, 2c, 2d, 2e)

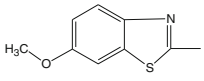

4. Conclusion

A series of Pd(II) complexes derived from 4-(4-alkoxy-2-hydroxybenzylideneamino)azobenzene with various alkoxy groups of even parity ($n = 8$–16) were successfully synthesized and characterized. All ligands and related Pd(II) complexes are enantiotropic. The ligands with flexible alkoxy chain $n = 8$ and $n = 10$ exhibit N and SmA phases while all the Pd(II) complexes show the SmA phase with the presence of arched shape during the cooling process. The melting and clearing temperatures of Pd(II) complexes are significantly higher as compared to the uncoordinated ligands and it is decreased with increase in length of the alkoxy chain. Besides, the Pd(II) complexes also have an exceptional higher phase transition temperatures as compared to Cu(II) and Ni(II) complexes. Comparative studies show that the azobenzene-cored Pd(II) complexes are more stable and favour the liquid crystalline formation as compared to the benzothiazole-cored Pd(II) complexes which are fully decomposed and non-mesogenic.

Acknowledgements

One of the authors (GYY) would like to thank Universiti Sains, Malaysia for the RU Grant No. 1001/PKIMIA/811223.

References

1. Meyer E, Zucco C and Gallarlo H 1998 *J. Mater. Chem*. **8** 1351
2. Thaker B T, Tander P K, Patel A S, Vyas C J, Jesani M S and Patel D M 2005 *Indian J. Chem*. **44A** 265
3. Chae H W, Kadhin O N and Choi M G 2009 *J. Liq. Cryst*. **36** 53
4. Huang K P, Misra T K, Wang G R, Huang B Y and Liu C Y 2008 *J. Chrom. A*. **1215** 177
5. Suste A and Sunjic V 1996 *Liq. Cryst*. **20** 219
6. Gayathri C and Ramalingan A 2008 *Spectrochim. Acta Mol. Biomol. Spectros*. **69** 980
7. Xu T, Zhang C, Lin Y and Qi S 2008 *Optical* **119** 643
8. Saad A, Galstyan T V, Denariez-Roberge M M and Dumont M 1998 *Optics Commun.* **151** 235
9. Rezvani Z, Ahar L R, Nejati K and Seyedahnadian S M 2004 *Acta Chim Slov*. **51** 675
10. Rezvani Z, Divband B, Abbasi A R and Nejati K 2006 *Polyhedron* **25** 1915
11. Nandiraju V S, Singha D, Das M and Paul M K 2002 *Mol. Cryst. Liq. Cryst*. **373** 105
12. Yeap G Y, Heng B T, Kakeya M, Takeuchi D, Gorecka E and Ito M M 2011 *J. Mol. Struct*. **999** 68
13. Yeap G Y, Heng B T, Tanabe M and Takeuchi D 2011 *Mol. Cryst. Liq. Cryst*. **552** 217
14. Pucci D, Aiello I, Bellusci A, Callipari G, Crispini A and Ghedini M 2009 *Mol. Cryst. Liq. Cryst*. **500** 144
15. Mustafaa I M, Hapipaha M A, Abdullab M A and Warda T R 2009 *Polyhedron* **28** 3993
16. Creavena B S, Duffa B, Egana D A, Kavanaghc K, Rosaird G, Thangellaa V R and Walsha M 2010 *Inorg. Chim. Acta* **363** 4048
17. Dey K, Sarkar S, Mukhopadhyay S, Malik A K, Biswas S and Bhaumik B B 2006 *J. Coord. Chem*. **11** 1233
18. Marcos M, Serrano J L, Sierra T and Gimenez 1993 *J. Chem. Mater*. **5** 1332
19. Yeap G Y, Ong C H, Takeuchi D, Kakeya M, Osakada K, Mahmood W A K, Atsuko O and Vill V 2008 *J. Mol. Struct*. **882** 18
20. Blackburn O A, Coe B J, Fielden J, Helliwell M, McDouall J W and Hutchings M G 2010 *Inorg. Chem*. **49** 9236
21. Hudson S A and Maitlis M 1993 *Chem. Rev*. **93** 861

22. Plasseraud L, Cuervo L G, Guillon D, Fink G S, Deschenaux R, Bruce DW and Donnio B 2002 *J. Mater. Chem*. **12** 2653
23. Karuna P, Reddy and Brown T R 1991 *J. Mater. Chem*. **1(5)** 757
24. Chae H W, Kadhin O N and Choi M G 2009 *J. Liq. Cryst*. **36** 53
25. Yeap G Y, Heng B T, Faradiana N, Zulkifly R, Ito M M, Tanabe M M and Takeuchi D 2012 *J. Mol. Struct*. **1012** 1